JOURNAL OF CATALYSIS **163,** 38–49 (1996)
ARTICLE NO. 0303

The Influence of Chelating Ligands on the Sulfidation of Ni and Mo in NiMo/SiO_2 Hydrotreating Catalysts

L. Medici and R. Prins*

Laboratorium für Technische Chemie, Eidgenössische Technische Hochschule, CH-8092 Zürich, Switzerland

Received October 30, 1995; revised March 18, 1996; accepted April 24, 1996

The influence of the addition of chelating ligands like nitrilotriacetic acid (NTA) during the preparation of NiMo/SiO_2 hydrotreating catalysts on catalyst activity and structure was studied by means of thiophene HDS (hydrodesulfurisation) activity measurements, temperature programmed sulfidation, and EXAFS (extended X-ray absorption fine structure) spectroscopy. The HDS activities of dried NiMo/SiO_2 catalysts prepared in the presence of NTA were much higher than those prepared by classic pore volume impregnation in the absence of NTA. Calcination led to sintering of the MoO_3 on the SiO_2 support, and thus to low HDS activities of the corresponding sulfided catalysts. After sulfidation at 493 K of dried but not calcined catalysts, molybdenum was fully sulfided, but not to MoS_2. The observed Mo–S and Mo–Mo distances pointed to Mo(V)–S_2–Mo(V) or Mo(IV)–S_2–Mo(IV) structures. MoS_2 was formed after sulfidation at 673 K, and its dispersion was independent of the presence of NTA in the original oxidic catalyst precursors. However, NTA had a dramatic influence on the sulfidation behavior of Ni. In the presence of NTA, Ni was sulfided between 493 and 583 K, while in its absence sulfidation started at temperatures below 493 K. It is proposed that the sulfidation of Ni at a relatively low temperature, before MoS_2 crystallites are formed, enhances the formation of thermodynamically stable nickel sulfides so that less of the HDS-active, but metastable, NiMoS phase can be formed. The role of NTA and similar chelating ligands is to prevent the sulfidation of nickel at low temperature, and thus increase the formation of the NiMoS phase.

INTRODUCTION

Industrial NiMo und CoMo hydrotreating catalysts are, without exception, supported on Al_2O_3, mainly because SiO_2-supported catalysts, prepared by conventional pore-filling impregnation and calcination, have a much lower hydrotreating activity (1). This has been ascribed to the low dispersion of the molybdenum and nickel oxides after calcination, and consequently to the low dispersion of MoS_2 and sulfided nickel on SiO_2 (1, 2). In the preceding article, we showed that it is the calcination stage which is responsible for this loss of dispersion (3). By adding chelating molecules like H_3NTA, nitrilotriacetic acid, and H_4EDTA, ethylenediamine tetraacetic acid, to the impregnation solution, and by leaving out the calcination step, it has, however, proved possible to prepare SiO_2-supported hydrotreating catalysts which have at least the same hydrotreating activity as their commercial γ-Al_2O_3 supported counterparts (1).

In the preceding paper (3), the structure of the Mo- and Ni-containing complexes present in the impregnation solution, as well as on the SiO_2 support after impregnation and drying, were studied by means of UV–VIS, Raman, IR, and X-ray absorption spectroscopy. It was found that, at a Ni : Mo : NTA = 0.5 : 1 : 1 molar ratio, all Ni ions are complexed with NTA. In solution $[Ni(NTA)(NH_3)_x(H_2O)_{2-x}]^-$ and $[Ni(NTA)_2]^{4-}$ complexes are present, depending on pH and concentrations. After drying on the SiO_2 support, only $[Ni(NTA)(H_2O)_2]^-$ and $[Ni(NTA)(SiO)_2]^{3-}$ complexes are present, the latter Ni(NTA) complex being bonded to the support through Ni–O–Si bonds. Because of the Ni : Mo : NTA = 0.5 : 1 : 1 stoichiometry and the complete complexation of Ni by NTA, about half of the Mo is present as $[MoO_3(NTA)]^{3-}$, and the other half as polymolybdate species. The polymolybdate was well dispersed and attached to the support by Si–O–Mo bonds.

The NiMo/SiO_2 catalyst, prepared by successive pore volume impregnations with solutions containing $Ni(NO_3)_2$ and $(NH_4)_6Mo_7O_{24}$ and drying, showed that when the first impregnation was done with the Ni-containing solution, $Ni(OH)_2$ crystallites formed on the SiO_2 surface, onto which MoO_4^{2-} ions grafted during the second impregnation with the Mo-containing solution. When the impregnation order was reversed, all Mo was present as well dispersed polymolybdate bonded through Si–O–Mo bonds to the support (3).

In the present work we will describe the sulfidation of the NTA-containing and classic catalysts. Sulfidation is an important step in catalyst preparation, since the activity of the working catalyst is known to depend on the mode of sulfidation (4). Whereas the structure of sulfided catalysts has been analysed in detail (5), interest in the way in which catalysts become sulfided has grown only in recent years. Temperature programmed sulfidation (TPS) studies (6–10)

* E-mail: prins@tech.chem.ethz.ch.

0021-9517/96 $18.00

especially, but also extended X-ray absorption fine structure (EXAFS) (11, 12), Mössbauer emission spectroscopy (13), laser Raman spectroscopy (14, 15), and XPS (16) studies have contributed to the understanding of sulfidation. In this study, the sulfidation process has been studied by TPS and EXAFS spectroscopy as a function of sulfidation temperature.

Hydrodesulfurisation (HDS) of thiophene is used in this work as a measure of the HDS activity of the catalysts studied. It will be shown that both the omission of the calcination step and the use of the NTA chelating agent are essential for attaining a good HDS activity for SiO_2-supported catalysts. The presence of the chelating ligand is most important, however, and the explanation for this is given.

EXPERIMENTAL

The TPS measurements and the thiophene HDS reactions occurred at atmospheric pressure in an apparatus which was a modified version of the flow system described in (17). He and H_2 were purified by feeding through a BTS and Pd/Al_2O_3 catalyst and 4-Å molecular sieves. A 10% H_2S in H_2 mixture (Union Carbide, 3.0) was used as received. The H_2 and 10% H_2S/H_2 flows were regulated with Brooks thermal mass flow controllers, whereas the He flow was controlled with a manual fine metering valve. A 3- and 4-way valve system allowed us to sulfide the catalyst in one reactor and simultaneously perform a thiophene HDS activity test in another.

The catalysts were prepared following a recipe in a European patent application (1). The Mo loadings of the samples containing NTA were kept constant at about 7.6% and 5.3% for the SiO_2 and Al_2O_3 supported catalysts, respectively. More details are given in the preceding paper (3). Prior to any HDS activity test, 100 mg of catalyst precursor was diluted with 1 g SiO_2 (C560 Chemie Uetikon) of the same particle size to avoid channeling effects and local temperature variations during sulfidation and HDS reaction, and then sulfided in a 60 ml/min flow of 10% H_2S/H_2 feed at 673 K (heating rate, 6 K/min) during 2 h. The feed, consisting of 6.5% thiophene in H_2, was obtained by bubbling H_2 through a series of 4 thiophene (Merck, for synthesis) saturators placed in a cryostat filled with a 1 : 1 mixture of H_2O and ethylene glycol cooled at 286.5 K. The catalyst testing temperature was at 673 K in all cases. The product stream was led to a Hewlett Packard HP 5890 gas chromatograph through a 125-ml sample loop, and a WCOT fused silica 0.25 mm × 50 m capillary column with a CP-SIL 5CB coating operated isothermally at 313 K was used for the analysis. The data were collected every 30 min with a Nelson Analytical intelligent interface (Perkin Elmer), and were transferred to an IBM PS2/80 computer, where the data analysis was performed with the Turbochrom 2700 version 3.2 (Perkin Elmer) program. The results after 3.5 h on stream were used for the determination of the kinetic parameters. The reaction rate was approximated with a first order expression in the thiophene partial pressure.

In the TPS measurements 200 mg catalyst was diluted with 1.8 g SiC (Lonza Carbomant 60S) instead of SiO_2 in order to avoid the physisorption of large amounts of H_2S during the sulfidation at room temperature. Prior to the TPS, the catalysts were dried *in situ* in a 30 ml/min He flow at 383 K for 1 h to eliminate adsorbed H_2O. The thermal conductivity of the feed gas (30 ml/min flow of 10% H_2S in H_2) was compared with that of the product stream at the end of the reactor by leading them through the reference and measuring channel of a Gow-Mac thermal conductivity detector (TCD) equipped with 4 WX filaments, held at 100 mA and 353 K. At the beginning of the measurement, the samples were held for 30 min at room temperature to stabilise the signal of the detector. Thereafter, the temperature was linearly raised to 873 K (heating rate, 6 K/min), and finally maintained at 873 K for another 30 min.

The sulfidation behavior of a NiMo(NTA)/SiO_2 0.5 : 1 : 1 catalyst prepared following the NTA-recipe (1) was analysed in detail by Ni and Mo *K*-edge EXAFS spectroscopy and compared with that of a NiMo/SiO_2 0.5 : 1 catalyst made by sequential impregnation of first the Ni and then the Mo salt. The EXAFS spectra were acquired on stations 8.1 and 9.2 at the SRS in Daresbury (UK). The synchrotron ring operated at an energy of 2 GeV and the electron current ranged between 120 and 250 mA.

The EXAFS data at the Mo and Ni *K*-edge were collected after drying the catalyst for 1 h at 383 K in a 30 ml/min He flow and subsequent sulfidation at room temperature for 30 min. Thereafter, the cell was flushed with a 60 ml/min flow of He to remove the excess H_2S, and the EXAFS measurements were performed in a He atmosphere at 120–140 K under liquid nitrogen cooling. After allowing the samples to warm up to room temperature, the sulfiding gas mixture was admitted again into the EXAFS cell and the catalysts were heated to 493 K (heating rate, 6 K/min). Immediately thereafter (without holding at 493 K), the H_2S/H_2 mixture was replaced by He and the cell was cooled to room temperature and closed. Again, EXAFS spectra were acquired at about 120–140K. For the NiMo(NTA)/SiO_2 0.5 : 1 : 1 catalyst, the sulfidation procedure was repeated at 583 K. Finally, EXAFS measurements were performed after sulfidation of the samples at 673 K (heating rate, 6 K/min) for 30 min and subsequent cooling to room temperature in a 60 ml/min He flow. For comparison, the Mo *K*-edge spectrum of a NiMo/SiO_2 0.5 : 1 catalyst, made by sequential impregnation of first the Mo and then the Ni salt, was also acquired after the same sulfidation procedure at 673 K. CoS_2, NiO, and $[P(C_6H_5)_4]_2[Ni(MoS_4)_2]$ were used as references for Ni–S, Ni–Ni, Ni–Mo, and Mo–Ni neighbors. The Mo–S and Mo–Mo contributions were fitted with the first Mo–S and Mo–Mo shells of MoS_2. Details of the EXAFS

measurements, the data analysis, and the experimental EXAFS references were published previously (17–19).

RESULTS

Thiophene HDS Activity

The activity of the NTA-based catalysts supported on SiO_2 and γ-Al_2O_3 is presented in Fig. 1 as a function of the Ni/Mo ratio. The catalyst activities increased with increasing Ni/Mo ratio due to the promoting effect of Ni, passed through a maximum around Ni/Mo = 0.3–0.4, and decreased at higher Ni/Mo ratios. Catalysts produced by EDTA were as good as those produced by NTA, at least up to Ni/Mo = 0.3. The catalysts supported on γ-Al_2O_3 had a lower activity than those on SiO_2, which might be due to a lower dispersion because of the lower surface area of γ-Al_2O_3, 235 m^2/g instead of 410 m^2/g for SiO_2 (the average mean pore diameters were 95 and 78 Å respectively).

The role of the different preparation procedures of the oxidic precursors was studied for SiO_2- and γ-Al_2O_3-supported catalysts at a constant Ni/Mo = 0.5 ratio (Table 1). The thiophene HDS activity increased in the order : calcined catalysts < dried catalysts < catalysts made in the presence of a chelating ligand. Differences between catalysts supported on γ-Al_2O_3 were smaller than differences between catalysts on SiO_2. On SiO_2, the catalysts prepared in the presence of chelating ligands were about three times more active than the calcined catalysts. Among the calcined and dried NiMo/SiO_2 catalysts, those prepared by sequential impregnation of first the Ni and then the Mo salt were clearly superior to their counterparts made in the reversed order, while the co-impregnated samples were in between.

NiMo(NTA)/SiO_2 catalysts with the molar ratio Ni : Mo : NTA = 0.5 : 1 : 1, and whose impregnating solutions had a pH varying from 6.0 to 9.0, all showed the same thiophene HDS activity. The same was true for two SiO_2-based catalysts made by sequential impregnation of first a Mo-and then a Ni-containing solution at their natural pH and at pH = 7.5. Apparently the pH of the impregnating solution does not have a strong influence on the formation of the catalytically active phase for pH values between 5 and 9. The pH at the precursor surface, and thus also the hydrolysis equilibria of the metal ions, are determined by the buffer capacity of the support and by the evaporation of part of the added NH_3 which also influences the pH of the support surface.

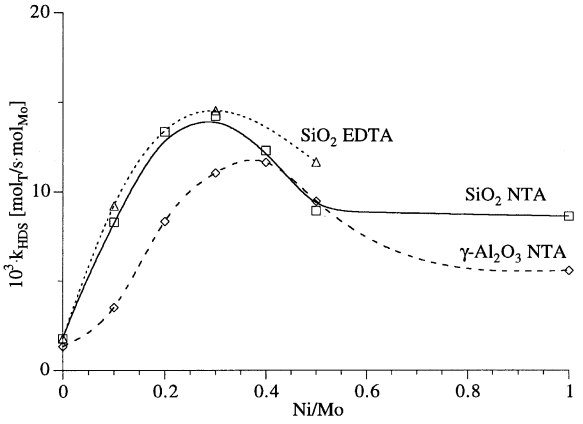

FIG. 1. Hydrodesulfurisation (HDS) activities of SiO_2- and γ-Al_2O_3-supported catalysts as a function of the Ni/Mo ratio and the chelating agent: SiO_2 EDTA (△ - - - △), SiO_2 NTA (□——□), γ-Al_2O_3 NTA (◇– – –◇).

SiO_2-supported NiMo catalysts with a Ni/Mo ratio of 0.3 showed behavior similar to those with Ni/Mo = 0.5. The thiophene HDS activities of the catalysts prepared in the presence of chelating ligands were higher than those at a Ni/Mo ratio of 0.5 (Fig. 1). The contrary was true for the other samples. Again, the calcined samples had a lower

TABLE 1

HDS Activities of NiMo Catalysts Supported on SiO_2 and γ-Al_2O_3 with Constant Ni/Mo = 0.5 Ratio as a Function of the Mode of Preparation

Impregnation mode	Calcination temperature [K]	Support	Mo loading [%]	$10^3 \cdot k_{HDS}$ [$mol_T/s \cdot mol_{Mo}$]
Mo first	673	SiO_2	7.53	3.3
Co-impregnation	673	SiO_2	7.47	3.3
Ni first	673	SiO_2	7.58	4.5
Mo first	n.c.[a]	SiO_2	7.52	4.8
Co-impregnation	n.c.	SiO_2	7.67	6.1
Ni first	n.c.	SiO_2	7.58	7.2
NTA	n.c.	SiO_2	7.58	10.1
EDTA	n.c.	SiO_2	7.54	11.7
Mo first	673	γ-Al_2O_3	4.5	7.4
Co-impregnation	n.c.	γ-Al_2O_3	4.96	8.3
Ni first	n.c.	γ-Al_2O_3	5.22	7.9
NTA	n.c.	γ-Al_2O_3	5.56	9.5

[a] n.c. = not calcined.

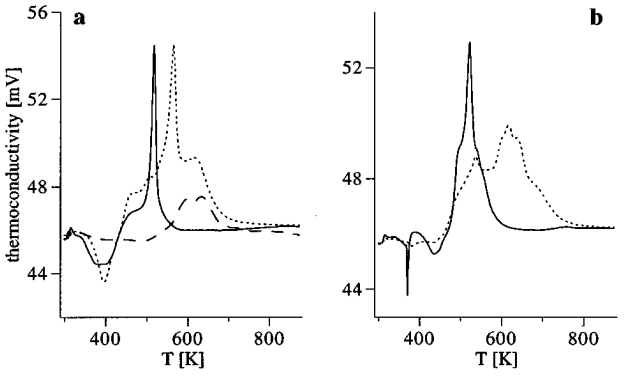

FIG. 2. Temperature-programmed sulfidation (TPS) patterns of Mo/SiO_2 (a) and Ni/SiO_2 catalysts (b) made with (- - -) and without (—) NTA addition compared with a blank NTA/SiO_2 sample (a) (– – –).

activity than the dried catalysts, and upon addition of chelating agents the activity improved by a factor of four.

The beneficial effect of the addition of NTA on the thiophene HDS activity was restricted to the catalysts containing both Ni and Mo. In fact, the HDS activities of the Mo/SiO_2 and Ni/SiO_2 catalysts did not change when NTA was added to their impregnating solutions. This suggests that NTA does not change the dispersion of the sulfide phases on the support surface directly. The role of the chelating ligands may instead be related to interactions between Ni and Mo during the sulfidation procedure, leading to a higher concentration of the "NiMoS" phase in the final operating state than in the samples prepared without addition of organic ligands.

Temperature Programmed Sulfidation

The TPS patterns of the catalysts containing only Mo or Ni with and without addition of NTA are shown in Fig. 2. An increase in the conductivity corresponds to H_2S production and/or H_2 consumption, and a negative peak to H_2S consumption and/or H_2 production. Because of the large H_2 excess ($H_2/H_2S = 9$, as in the sulfidation preceding the HDS tests), this experimental setup was more sensitive to variations in the H_2S than in the H_2 concentration. The H_2S consumption peak between 320 and 450 K in the sulfidation of the Mo/SiO_2 catalyst (Fig. 2a) is attributed (7) to an oxygen–sulfur exchange reaction on the surface of the well-dispersed polymolybdates present in the dried state (3). According to the literature (12, 14–16, 20), during this process molybdenum is reduced and disulfide ligands are formed. Finally, the molybdenum sulfide species are reduced to MoS_2 at 520 K, where a large H_2S production was observed (Fig. 2a). The addition of NTA changed the sulfidation strongly. The H_2S consumption peak of the $Mo(NTA)/SiO_2$ catalyst at 395 K was sharper and slightly shifted to higher temperatures, suggesting that the Mo structure was more uniform and more stable than in the NTA-free case. The main H_2S production and/or H_2 consumption peak was shifted to 565 K and had a shoulder at 620 K. A separate experiment with a NTA/SiO_2 sample showed that the shoulder is due to the reduction of the chelating ligand. The shift of the reduction peak from 520 to 565 K might be due to a retarded reduction of the species with MoS_3 stoichiometry because of a stabilisation by NTA.

The sulfidation of the Ni/SiO_2 catalyst was more complex (Fig. 2b), since an additional sharp H_2S consumption peak was found at 370 K which was not present in the TPS patterns of the $Ni(NO_3)_2 \cdot 6H_2O$ reference compound and of the calcined Co/Al_2O_3 samples studied by Arnoldy *et al.* (8). The reduction peak at 525 K is probably due to the reduction of elemental sulfur formed on the surface of the catalyst during the oxygen–sulfur exchange reaction and coupled redox reaction (8). Despite the high Ni loading, the $Ni(NTA)/SiO_2$ catalyst showed no significant H_2S consumption over the whole temperature range between 300 and 900 K (Fig. 2b). The TPS pattern is dominated by the combined sulfidation of Ni and the reduction of NTA between 500 and 700 K, with an additional peak at 540 K whose origin is not clear. Probably, the negative peak of the sulfidation of Ni is overshadowed by the positive peak of the reductive decomposition of the NTA ligands.

The TPS patterns of oxidic $NiMo/SiO_2$ catalysts which were calcined at 673 K after the second impregnation deviated only slightly from a straight line (Fig. 3a). Like Arnoldy *et al.* (7) for bulk MoO_3 and Scheffer *et al.* (10) for calcined Mo/SiO_2 samples, we attribute this to the presence of large MoO_3 crystals in the calcined $NiMo/SiO_2$ catalysts. It explains why these catalysts had a low HDS activity (Table 1).

All dried samples had similar TPS patterns, with one or more H_2S consumption peaks below 500 K and a quite

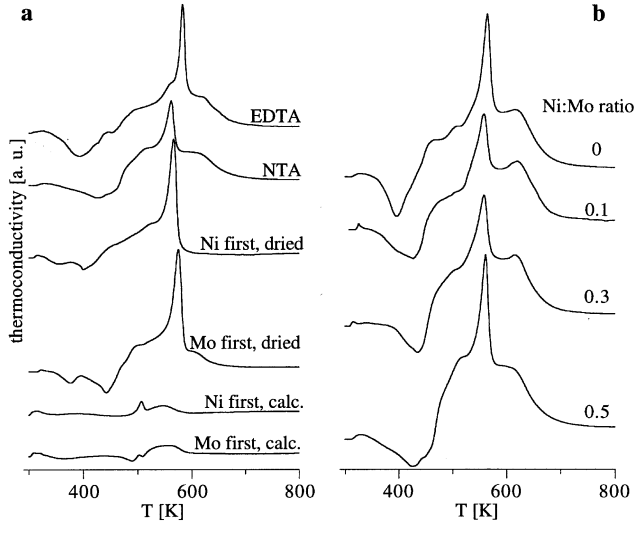

FIG. 3. (a) TPS patterns of $NiMo/SiO_2$ catalysts with constant $Ni/Mo = 0.5$ ratio as a function of the preparation mode. (b) TPS patterns of $NiMo(NTA)/SiO_2$ catalysts with varying Ni/Mo ratio.

large reduction peak between 560 and 580 K (Fig. 3a). The $NiMo/SiO_2$ catalyst made by sequential impregnation of first Mo and then Ni showed two H_2S consumption peaks at 375 and 440 K which are attributed to the separate sulfidation of Mo and Ni respectively, as in the Mo/SiO_2 and Ni/SiO_2 samples (Fig. 2). This is in accordance with the proposed structure of this dried catalyst, in which Ni is supposed to be present as $Ni(NO_3)_2$, and Mo as well dispersed molybdate in contact with the SiO_2 surface or, partly, as 12-molybdosilicic acid fragments, as in the dried Mo/SiO_2 catalyst (3). The large H_2S production peak at 575 K and the shoulder at 610 K indicate that the MoS_3-like intermediate is reduced to MoS_2 at a higher temperature when Ni is present.

The TPS pattern of the $NiMo/SiO_2$ (Ni-first, dried) catalyst differs from that of the Mo-first, dried catalyst by a shift of the H_2S consumption peaks and the reduction peak to lower temperatures and by the absence of the shoulder at 610 K (Fig. 3a). Because of the structural differences in the dried state (3), this is not unexpected.

The general appearance of the TPS pattern of the $NiMo(NTA)/SiO_2$ catalyst is similar to that of the $Mo(NTA)/SiO_2$ catalyst (Fig. 3b), but there are differences in the sulfidation at low temperature and in the intensity of the shoulder at 620 K. Mo is present in the dried catalyst precursor as a mixture of $[MoO_3(NTA)]^{3-}$ and probably fragments of 12-molybdosilicic acid (3). The observed TPS pattern is therefore most likely a superposition of the sulfidation of polymolybdates in the presence of Ni, and of the $[MoO_3(NTA)]^{3-}$ and $[Ni(NTA)(H_2O)_2]^{-}$ complexes. The TPS of the $NiMo(EDTA)/SiO_2$ 0.5 : 1 : 0.5 catalyst looks similar to that of the NTA-based counterpart (Fig. 3a), although the H_2S consumption minimum has shifted from 425 to 390 K and the reduction peak from 560 to 580 K.

To investigate whether Ni is still complexed with NTA during the sulfidation, the TPS profiles of $NiMo(NTA)/SiO_2$ catalysts were measured as a function of the Ni/Mo ratio (Fig. 3b). The H_2S consumption peak already shifted from 395 to 425 K after addition of 0.1 equivalent Ni per Mo, but did not shift further at higher Ni/Mo ratios. The peak width increased with increasing Ni/Mo ratio. The reduction peak remained at 560 K independent of the Ni/Mo ratio. This shows that the characteristic features of the sulfidation of the $[MoO_3(NTA)]^{3-}$ complex are gradually replaced by those of the molybdates, as present in the TPS profiles of Mo/SiO_2 and $NiMo/SiO_2$ (Mo-first, dried) catalysts. On the other hand, the absence of a second H_2S consumption peak around 400 K suggests that Ni is still bound to NTA during the sulfidation until NTA is reduced, as observed for the Ni/SiO_2 catalyst (Fig. 2b).

The TPS measurements show that both Ni and NTA shift the reduction temperature of the MoS_3-like phase by 40–50 K to higher temperatures. The reason for this effect, which is even stronger for EDTA-based catalysts ($\Delta T = 60$ K), is not clear. It could be due to interactions of the MoS_3-like intermediate with the ligands which are still present on the catalyst surface up to 600 K and with Ni ions.

Molybdenum X-Ray Absorption Spectroscopy

Based on the TPS results, it was decided to perform a Ni and Mo *K*-edge EXAFS analysis of the $NiMo(NTA)/SiO_2$ catalyst and the $NiMo/SiO_2$ (Ni-first, dried) catalyst, which was the most active among the dried catalysts prepared without addition of chelating ligands. Both catalysts had a Ni/Mo = 0.5 ratio. EXAFS spectra were taken after 30 min of sulfidation at room temperature, which allowed us to check whether the samples were already partially sulfided, as suggested in the literature based on color changes after exposure of the catalysts to H_2S/H_2 mixtures (6–10).

The EXAFS spectra were also measured after sulfidation at 493 K, before the combined H_2S production and H_2 consumption around 560 K took place in the TPS profiles. The EXAFS spectra of the NTA-based sample were furthermore collected after treatment at 583 K, after the TPS reduction peak. Finally, spectra were measured after sulfidation at 673 K, the final sulfidation temperature at which the catalysts were treated prior to the thiophene HDS experiments. The Fourier transformations of the $\chi(k) \cdot k^3$ Mo EXAFS spectra in the range $3.2 \leq k \leq 19.7$ Å^{-1} are presented in Fig. 4.

The oxidic Mo species are mainly present as molybdates on the surface of the $Ni(OH)_2$ crystallites in the $NiMo/SiO_2$ (Ni-first) catalyst and as a mixture of the $[MoO_3(NTA)]^{3-}$ complex and fragments of 12-molybdosilicic acid or molyb-

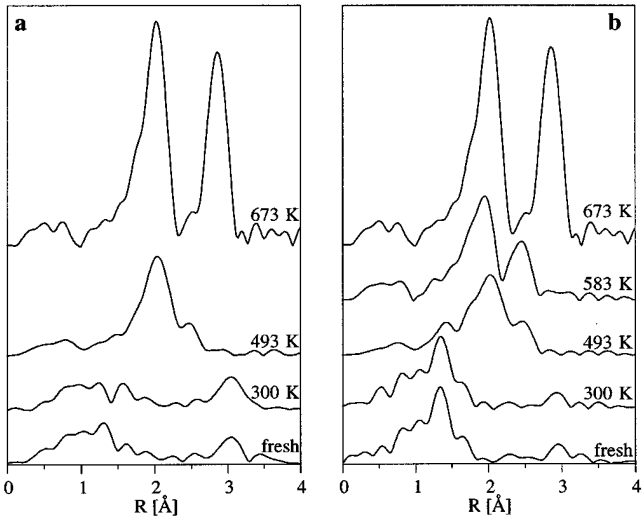

FIG. 4. Absolute values of the Mo *K*-edge $\chi(k) \cdot k^3$ Fourier transformed spectra of the $NiMo/SiO_2$ (a) and $NiMo(NTA)/SiO_2$ (b) catalysts (both with Ni/Mo = 0.5) as a function of the pretreatment. From bottom to top are shown fresh dried catalysts and samples sulfided at 300, 493, 583, and 673 K.

TABLE 2

Fits of the Mo *K*-Edge Fourier-Filtered $\chi(k) \cdot k^3$ EXAFS of the Dried NiMo/SiO_2 Catalysts as a Function of the Preparation Mode and of the Sulfiding Temperature

Impregnation mode	Sulf. temp. [K]	Shell	N_{coord}	R [Å]	$\Delta\sigma^2$ [Å^2]	ΔE_0 [eV]	k-range [Å^{-1}]	R-range [Å]
Ni first	493	S	4.0	2.46	0.0024	−1.2	3.0–15.3	1.04–3.05
		Mo	0.2	2.78	−0.0008	−7.8		
NTA	493	O	0.3	1.71	−0.0003	−19.7	3.0–14.5	1.02–2.89
		S	4.5	2.45	0.0057	−2.7		
		Mo	1.1	2.74	0.0042	8.6		
NTA	583	S	4.7	2.37	0.0039	3.4	3.0–18.0	0.98–2.68
		Mo	1.1	2.76	0.0021	6.6		
Ni first	673	S	6	2.41	0.0006	0	3.0–19.8	0.97–3.25
		Mo	3.4	3.16	0.0008	−1		
NTA	673	S	6.3	2.41	0.0008	−0.2	3.0–19.9	0.97–3.27
		Mo	3.1	3.16	0.0005	−0.5		
Mo first	673	S	6.2	2.41	0.0008	−0.2	3.0–19.8	0.99–3.30
		Mo	3.1	3.16	0.0004	−0.6		

dates adsorbed on the SiO_2 surface in the NiMo(NTA)/SiO_2 catalyst (3). The Mo *K*-edge spectra of both catalysts changed completely when the sulfidation temperature was increased from room temperature to 493 K, and changed again upon further increase to 673 K. In contrast, the H_2S/H_2 treatment at 300 K did not affect the features of the absolute part of the Fourier transformations very much. The amplitude of the broad Mo–O peak with maximum at 1.3 Å of the NiMo/SiO_2 (Ni-first) catalyst decreased (Fig. 4a), and the intensity of the contribution at 3.05 Å, due to Ni backscatterers in the dried sample (3), as well as the intensity of the peak at 1.55 Å increased. The latter was associated with a slight change of the imaginary part of the Fourier transformation, suggesting that sulfur atoms at about 2.2 Å from the Mo atoms replaced the oxygen atoms of the molybdates. Such a distance is characteristic for a Mo–S bond with a π contribution, like a terminal Mo=S bond. Note that the distances observed in the Fourier-transformed spectra are always shorter than the real absorber–backscatterer distances because of the phase shift. In contrast, the spectrum of the NTA-based counterpart remained unchanged during sulfidation at 300 K. Apparently, the presence of NTA hinders or substantially slows down the sulfidation of the oxidic Mo species at room temperature, due to the partial formation of the $[MoO_3(NTA)]^{3-}$ complex as well as to other interactions of the Mo atoms with the chelating ligand.

The Mo *K*-edge EXAFS spectrum of the NiMo/SiO_2 catalyst after sulfidation at 493 K was completely different from that of the dried precursor (Fig. 4a). All oxygen contributions between 1 and 1.5 Å had disappeared, and a new peak at 2.05 Å with a sideband at 2.45 Å had appeared. The NiMo(NTA)/SiO_2 catalyst experienced a similar change, although a small peak at 1.4 Å remained after sulfidation at 493 K (Fig. 4b). Long range order beyond 3 Å was absent in both samples. The $\chi(k) \cdot k^3$ Fourier transformations of the NiMo/SiO_2 and NiMo(NTA)/SiO_2 catalysts differed mainly in their absolute parts, whereas the imaginary parts were quite similar over the whole spectrum, indicating that the same Mo neighbors were present in both samples. A quantitative analysis of the EXAFS spectra after sulfidation at 493 K was made. The main contributions in both fits were sulfur neighbors at about 2.45 Å and molybdenum backscatterers at about 2.76 Å (Table 2). In the NiMo/SiO_2 (Ni-first) catalyst, every Mo possessed 4 S neighbors at 2.46 Å and 0.2 Mo backscatterers at 2.78 Å (Table 2 and Fig. 5). The significance of the fit and especially that of the very small Mo–Mo contribution were checked with *F*-tests (21) using the residual square sum of the $\chi(k) \cdot k^3$ regression curve as the estimate for the statistical error of the data ($\Gamma(\text{tot}) = 363 > F_{0.95}(8, 7) = 3.7$ and $\Gamma(\text{S} + \text{Mo}) = 18.9 > F_{0.95}(4, 7) = 4.1$, respectively). Γ(tot) is the ratio between the average regression square sum for every parameter and the statistical error. For the significance test of a new shell, $\Gamma(\text{S} + \text{Mo})$ compares the improvement of the regression square sum with the loss of four degrees of freedom. To obtain a better fit at small distances, we also tried to add an oxygen contribution around 1.7 Å, but the improvement was marginal.

In the Fourier transformed spectrum of the NiMo(NTA)/SiO_2 catalyst after sulfidation at 493 K (Fig. 4b), oxygen backscatterers at the same position as the main Mo–O peak in the dried sample could clearly be observed. In fact, the two-shell fit with sulfur at 2.45 Å and

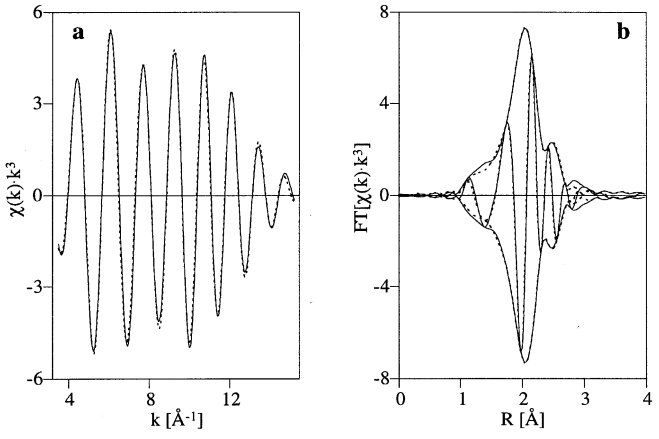

FIG. 5. Mo *K*-edge Fourier-filtered data (—) and corresponding two-shell fit (- - -) of the $NiMo/SiO_2$ (Ni-first, dried) catalyst sulfided at 493 K: $\chi(k) \cdot k^3$ (a) and k^3-Fourier transformation (b).

molybdenum at 2.74 Å could be improved significantly by an additional oxygen contribution at 1.71 Å (the percentage of the total square sum explained by the fit increased from 97.5 to 99.6%), although the energy origin correction was unusually strongly negative (Table 2).

The EXAFS spectra of the samples sulfided at 493 K are different from those of hydrotreating catalysts sulfided at 673 K and of MoS_2, because of the absence of the strong Mo–Mo contribution at 3.15 Å (18, 22). They are, however, very similar to the EXAFS spectrum presented by Cramer *et al.* (23) for the $[Mo_2(S_2)_6]^{2-}$ anion, although the Mo–S coordination numbers of 4–4.5 for the first shell at 2.45 Å are only half of the crystallographic value for the $[Mo_2(S_2)_6]^{2-}$ complex (24). The Mo–S and Mo–Mo distances of 2.45 and 2.76 Å, respectively, are to be expected for Mo(V)–S_2–Mo(V) fragments (25).

Also, after sulfidation at 583 K, the Fourier transformed spectrum of the $NiMo(NTA)/SiO_2$ catalyst did not yet resemble that of MoS_2, although this temperature was higher than that of the reduction peak at 560 K in the TPS measurements (Fig. 3). The Mo–Mo peak had the same imaginary part but a larger amplitude than that in the sample sulfided at 493 K, while the main Mo–S peak was slightly shifted toward shorter distances and the Mo–O contribution had disappeared completely (Fig. 4b). The fit of these Fourier filtered data delivered similar coordination numbers but smaller Debye–Waller factors than the sample sulfided at 493 K (Table 2). The main difference was the shift of the Mo–S contribution from 2.45 to 2.37 Å, which is between Mo and the bridging sulfur atom in the $[Mo_3S(S_2)_6]^{2-}$ cluster anion (26) but which could not be detected in the Mo *K*-edge EXAFS of its ammonium salt (23). Although the total fit and the Mo–Mo contribution were statistically significant ($\Gamma(\text{tot}) = 58.2 > F_{0.95}(8, 8) = 3.4$ and $\Gamma(\text{S} + \text{Mo}) = 23.4 > F_{0.95}(4, 8) = 3.8$), the fit quality was not as good as for the preceding samples. This may be due to the presence of some MoS_2, formed in the phase transition from the MoS_3-like phase to MoS_2 which is supposed to occur in this temperature region (Fig. 3).

Although the thiophene HDS activities of the $NiMo/SiO_2$ (Ni-first, dried) and the $NiMo(NTA)/SiO_2$ catalysts were different (Table 1), their EXAFS spectra after sulfidation at 673 K were identical within the uncertainty of the measurement, and also identical to that of the $NiMo/SiO_2$ (Mo-first, dried) catalyst (Fig. 6). The results of the fitting in Table 2 and the results of the *F*-tests on the fits confirmed that the MoS_2 dispersions in the three sulfided catalysts are equal. The first Mo–S and the Mo–Mo coordination distances of these three samples are identical and equal to those known for MoS_2 (22). The Mo–Mo coordination numbers are comparable to those measured for small MoS_2 crystallites in similarly prepared catalysts (some also prepared by adding the chelating ligand NTA) and supported on γ-Al_2O_3, SiO_2, and active carbon (18, 27). From the relation between the Mo–Mo coordination number and the number of Mo atoms in the MoS_2 crystallites (18), it is concluded that the MoS_2 slabs contain about 6–7 Mo atoms. A Mo–S coordination number of 4.7 is predicted for such small electroneutral MoS_2 slabs if they contain only Mo^{4+} and S^{2-} ions. This is much smaller than the observed coordination number (Table 2). The Mo coordination number may be increased (while keeping the MoS_2 crystallites electroneutral) by the presence of S_2^{2-} instead of S^{2-} anions at the edges due to the treatment in 10% H_2S/H_2, or by the presence of Ni and S in the "NiMoS" phase on the edges of the MoS_2 crystallites. The sulfur corresponding to the Ni may complete the coordination sphere of the Mo atoms and thus be responsible for the Mo–S coordination number of 6 found for the catalysts sulfided at 673 K.

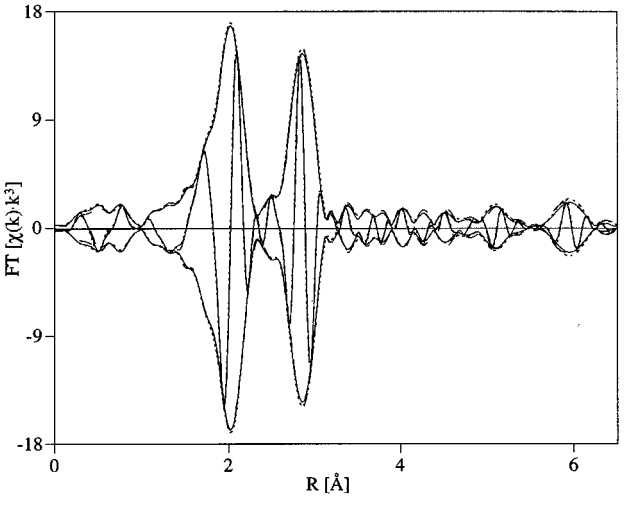

FIG. 6. Mo *K*-edge $\chi(k) \cdot k^3$ Fourier transformed spectra of dried $NiMo/SiO_2$ catalysts sulfided at 673 K: Ni-first (—), NTA (- - -), and Mo-first (– – –).

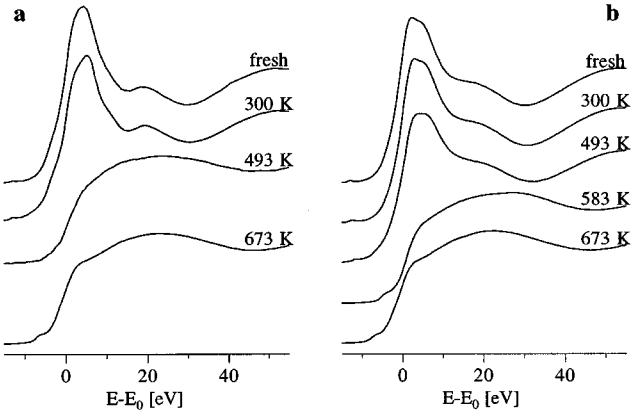

FIG. 7. Normalised, pre-edge subtracted Ni *K*-edge XANES spectra of the NiMo/SiO_2 (Ni-first, dried) (a) and NiMo(NTA)/SiO_2 (b) catalysts as a function of the pretreatment (both with Ni/Mo = 0.5). From top to bottom are shown fresh dried catalysts and samples sulfided at 300, 493, 583, and 673 K.

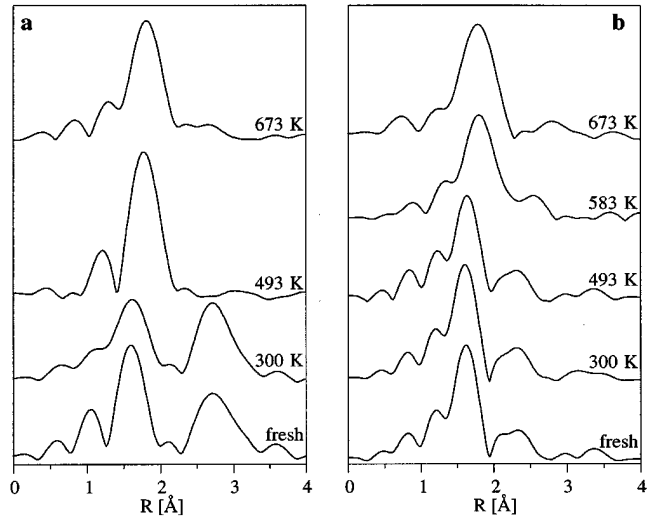

FIG. 8. Absolute values of the Ni *K*-edge $\chi(k)\cdot k^3$ Fourier-transformed spectra of the NiMo/SiO_2 (a) and NiMo(NTA)/SiO_2 (b) catalysts (both with Ni/Mo = 0.5) as a function of the pretreatment. From bottom to top are shown fresh dried catalysts and samples sulfided at 300, 493, 583, and 673 K.

Nickel X-Ray Absorption Spectroscopy

NiMo/SiO_2 (Ni-first) and NiMo(NTA)/SiO_2 samples with Ni/Mo = 0.5 prepared in the same manner as for the foregoing Mo XAS measurements were analysed at the Ni *K*-edge to investigate the influence of the NTA chelating ligand on the sulfidation behavior of Ni. Figure 7 shows the Ni *K* absorption edges as a function of the sulfidation temperature. The shape of the white line had changed somewhat after 30 min of sulfidation of the NiMo/SiO_2 catalyst at 300 K, and no white line was detected after sulfidation at 493 K. In contrast, the X-ray absorption near edge spectrum (XANES) of the NiMo(NTA)/SiO_2 catalyst after sulfidation at room temperature was identical to that of the fresh catalyst, while after treatment at 493 K the white line had only changed slightly (Fig. 7b). After sulfidation at 583 K, the white line had disappeared, indicating that the Ni in the NiMo(NTA)/SiO_2 catalyst had been sulfided completely. The sulfur atoms around Ni in the NiMo/SiO_2 catalyst after sulfidation at 493 K must be coordinated in a different way than in the NiMo(NTA)/SiO_2 catalyst after sulfidation at 583 K, since a small pre-edge feature at −4 eV was observed for the latter catalyst whereas for the former it was completely absent. This pre-edge peak is due to the $1s \rightarrow 3d$ transition in sites of low symmetry. After 30 min of sulfidation at 673 K, both catalysts had similar XANES spectra, including the pre-edge peak and a band at 2–3 eV due to the $1s \rightarrow 4p$ transition, as in several bulk sulfide Ni and Co reference compounds (28, 29).

The XANES results were confirmed by the Ni *K*-edge Fourier transformed EXAFS spectra shown in Fig. 8. The sulfidation of the NiMo/SiO_2 catalyst at room temperature caused a decrease in the amplitude of the Ni–O contribution at 1.6 Å, but no shift of the corresponding imaginary part nor an appearance of a new Ni–S peak (Fig. 9a). On the other hand, the intensity of the peak at 2.7 Å which was fitted with a Ni–Ni shell at 3.13 Å for the dried sample (3), increased by about 10% compared with the fresh catalyst (Fig. 9a). The change might come from the partial exchange of oxygen atoms at the $Ni(OH)_2$ surface by sulfur atoms arranged in a disordered mode.

After treatment at 493 K, the main peak had shifted from 1.6 to 1.75 Å and other signals had disappeared (Fig. 8a). A strong sidelobe appeared at 1.2 Å which was reproduced in two independent experiments at stations 8.1 and 9.2, although it is impossible to arrange oxygen or sulfur neighbors at such a short distance from the Ni^{2+} center. On the contrary, for the NiMo(NTA)/SiO_2 catalyst hardly any

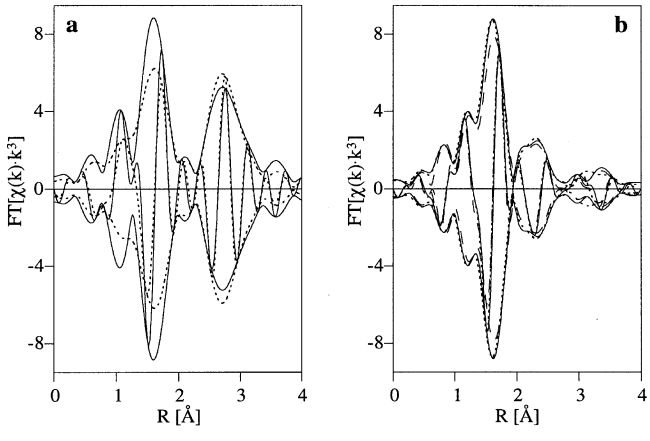

FIG. 9. Ni *K*-edge $\chi(k)\cdot k^3$ Fourier transformed spectra of the NiMo/SiO_2 (a) and NiMo(NTA)/SiO_2 (b) catalysts as a function of pretreatment: Fresh dried catalysts (—), and samples sulfided at 300 (- - -) and 493 (– – –) K.

TABLE 3

Fits of the Ni *K*-Edge Fourier Filtered $\chi(k)\cdot k^3$ EXAFS of the Dried NiMo/SiO_2 Catalysts as a Function of the Preparation Mode and of the Sulfiding Temperature

Impregnation mode	Sulf. temp. [K]	Shell	N_{coord}	R [Å]	$\Delta\sigma^2$ [Å^2]	ΔE_0 [eV]	k-range [Å^{-1}]	R-range [Å]
Ni first	493	S	4.6	2.22	−0.0006	6	3.0–12.1	0.82–2.47
NTA	583	S	6.7	2.24	0.0055	2.1	3.1–13.0	1.05–2.84
		Ni	1.2	2.81	0.0011	6.7		
Ni first	673	S	5.1	2.23	0.0021	4.2	3.0–12.8	1.02–3.07
		Ni	0.5	2.53	0.001	−4.8		
		Mo	0.8	2.85	0.0042	−13.2		
NTA	673	S	6.0	2.23	0.0029	3.7	3.0–10.9	0.97–3.37
		Mo	1.0	2.85	0.0062	−18.5		
		S	0.7	3.19	−0.001	5		

differences between the fresh sample and the samples sulfided at room temperature and 493 K were observed (Figs. 8b and 9b), in agreement with the XANES spectra (Fig. 7b). The fitting procedure for the Ni EXAFS data of the NiMo/SiO_2 (Ni-first) catalyst sulfided at 493 K after Fourier filtering delivered a negative Debye–Waller factor and an unexpectedly small Ni–S coordination number of 4.6 (Table 3) compared with that of a CoMo/C catalyst treated at 473 K (11). Due to the presence of the curious sidelobe at 1.2 Å, it was not possible to improve the fit by adding another shell.

Like the Ni *K*-edge XANES spectrum (Fig. 7b), the EXAFS spectra (Fig. 8b) of the NiMo(NTA)/SiO_2 catalyst changed completely after sulfidation at 583 K. The main peak of the Fourier transformed spectrum was at 1.8 Å, the same as for the NiMo/SiO_2 catalyst sulfided at 493 K (Fig. 8), confirming that oxygen was substituted by sulfur in the coordination sphere of Ni. The parameters obtained from the fitting procedure of the Fourier filtered data are listed in Table 3. As expected, the main contribution was a Ni–S coordination at 2.24 Å. The presence of a Ni–Ni shell at 2.81 Å is in agreement with the results observed for a CoMo/C catalyst after sulfidation to 573 K (11). Fits of the second shell with a Ni–Mo contribution at 2.8 Å or a Ni–Ni coordination at 2.5 Å, as in Ni_3S_2 (30), were unsuccessful.

The increase in the sulfidation temperature from 493 to 673 K for the NiMo/SiO_2 catalyst caused a decrease in the intensity of the Ni–S contribution and the disappearance of the sidelobe at 1.2 Å, while a new small peak appeared at 2.6 Å (Fig. 8a). The position and amplitude of the Ni–S peak in the Fourier transformation of the NiMo(NTA)/SiO_2 catalyst hardly changed after H_2S/H_2 treatment at 673 K, whereas the peak at 2.6 Å in the pseudo-radial distribution attributed to a Ni–Ni distance of 2.8 Å was replaced by a new one at 2.8 Å (Fig. 8b). After 30 min of sulfidation at 673 K, the Ni *K*-edge spectra of the NiMo/SiO_2 and NiMo(NTA)/SiO_2 catalysts were very similar (Fig. 8), except for the small features above 2.5 Å which are partly caused by the different ranges of the Fourier transformations, because the spectrum of the NTA sample had to be truncated at 10.9 Å^{-1} due to the bad data quality at higher k-values (Table 3). In fact, the differences between the spectra became negligible when the k-region for the Fourier transformation of the $\chi(k)\cdot k^3$ of the NiMo/SiO_2 catalyst was also truncated at 10.9 Å^{-1}, except for the absolute and imaginary parts around 2.3 Å.

Fourier filtering and fitting of the data led to the parameters listed in Table 3. Comparisons between data and corresponding fits in both k^1- and k^3-Fourier transformed space for the NiMo/SiO_2 (Ni-first) catalyst are presented in Fig. 10; they show a good agreement in the range between 1.5 and 3 Å. Ni has six sulfur neighbors and one molybdenum neighbor at 2.23 and 2.85 Å, respectively, in the NiMo(NTA)/SiO_2 catalyst. An additional Ni–S shell was added to improve the fit quality around 3 Å. The Ni–S coordination number of six is indicative of coordinatively

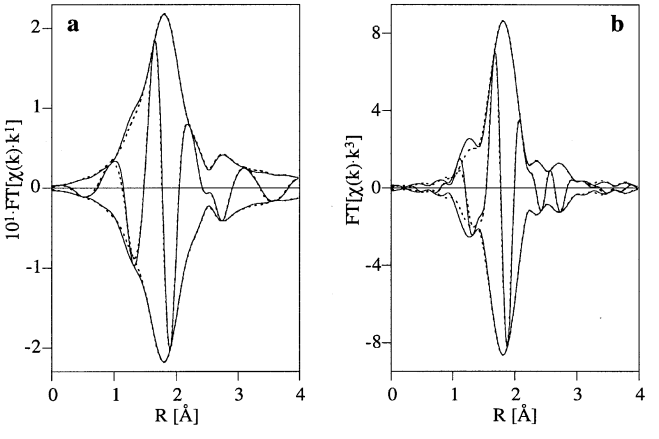

FIG. 10. Ni *K*-edge $\chi(k)\cdot k^3$ Fourier-filtered data (—) and corresponding fit (- - -) of the NiMo/SiO_2 (Ni-first, dried) catalyst sulfided at 673 K: $\chi(k)\cdot k^1$ (a) and $\chi(k)\cdot k^3$-Fourier transforms (b).

saturated Ni atoms in the "NiMoS" phase. This relatively high number is probably caused by the sulfidation treatment, in which the sample was held during 30 min in a 10% H_2S in H_2 mixture at 673 K prior to cooling to room temperature in a He atmosphere. Bouwens *et al*. (18, 31) and Louwers and Prins (17) flushed their samples with He at 673 K for 30 min prior to cooling and eliminated thereby part of the sulfur from the catalysts. Their Ni–S coordination numbers were close to 5. The same Ni–S and Ni–Mo distances as found for the NiMo(NTA)/SiO_2 catalyst were also observed for the NiMo/SiO_2 catalyst; the corresponding coordination numbers of 5.1 and 0.8, respectively, were somewhat smaller. A Ni–Ni contribution at 2.53 Å suggests that small Ni_3S_2 crystallites are present in the NiMo/SiO_2 catalyst in addition to the "NiMoS" phase, since a Ni–Ni coordination at 2.50 Å exists in bulk Ni_3S_2 (30). Since the overall Ni–S coordination number of 5.1 obtained for the NiMo/SiO_2 catalyst is an average between the coordination numbers of the "NiMoS" phase and the Ni_3S_2 crystallites (in which each Ni atom has four sulfur neighbors at 2.28 Å (30)), the Ni–S coordination number of the Ni atoms in the "NiMoS" phase should be higher than 5.1 and probably is similar to that in the NiMo(NTA)/SiO_2 catalyst.

The strongly negative corrections for the energy origin of the Ni–Mo shells of both catalysts (Table 3) are partly due to their correlation with the estimate of the Ni–Mo distance. Nevertheless, negative ΔE_0 values were reported before for NiMo, CoMo, and NiW catalysts (11, 17, 27, 29, 31, 32). This could be due to the different chemical environments in the sulfided hydrotreating catalysts and the $[(C_6H_5)_4P]_2[Ni(MS_4)_2]$ reference complexes ($M =$ Mo or W), especially the different oxidation states of the Mo and W atoms (VI in the complex and IV in the sulfided catalysts).

DISCUSSION

The SiO_2-supported catalysts which were calcined at 673 K did not show any significant peak in the TPS patterns (Fig. 3) and had a low thiophene HDS activity compared with the γ-Al_2O_3 catalysts (Table 1). Both features are caused by the weak interactions between molybdates and SiO_2 surface ((3) and references therein). Therefore, large MoO_3 crystallites are formed during calcination, and their sulfidation is similar to that of bulk MoO_3 (7). H_2S may cause an oxygen–sulfur exchange on the surface of MoO_3 at moderate temperatures (16), leading to Mo oxysulfide which should facilitate the bulk reduction of MoO_3 to MoO_2(7). As a redispersion of the Mo phase is not likely to take place, the MoS_2 crystallites should be very large and have a low intrinsic HDS activity. In addition, they cannot accommodate much Ni in the "NiMoS" phase on the edges due to the low specific surface area, and thus they have a low catalytic performance.

The TPS patterns of the dried catalysts, which for CoMo/Al_2O_3 catalysts depended mainly on the sulfidation of Mo (6), were very different from those of the calcined samples and did not show much dependence on the Ni/Mo ratio. The TPS peaks were all shifted compared with those of the Mo-only catalyst (cf. Figs. 2 and 3) due to the presence of Ni.

Sulfidation of the Mo phase of the NiMo/SiO_2 and NiMo(NTA)/SiO_2 catalysts at room temperature hardly took place, as demonstrated by the Mo EXAFS spectra which were still similar to those of the fresh catalysts (Fig. 4). After treatment at 493 K, the Mo–S and Mo–Mo distances were equivalent to those reported by de Boer *et al*. (12) for a calcined, well dispersed MoO_3/SiO_2 catalyst prepared from a solution containing trivalent Mo species by deposition–precipitation. This catalyst had been sulfided for 30 min at 423 K, and the Mo–S and Mo–Mo distances were claimed to correspond to those of MoS_3. On the contrary, the Mo–S and Mo–Mo coordination numbers obtained in the present study did not agree with the values of MoS_3 (25), which was only partly due to the incomplete sulfidation of the NiMo(NTA)/SiO_2 catalyst. It is not clear whether this difference is due to the presence of Ni, to the lack of calcination, or more probably to the higher dispersion of the present samples which showed very small Mo–Mo coordination in the dried state, if any (compare (3) with the analysis of the MoO_3/SiO_2 samples in the oxidic state (33)). After the molybdate ions adsorbed on the SiO_2 surface had exchanged their oxygen atoms for sulfur, they probably did not sinter to bulk MoS_3 but formed small MoS_3-like clusters containing only a few Mo atoms, although the interactions between Mo and support are small (34). Their structure may be analogous to that of the $[Mo_2(S_2)_6]^{2-}$ complex, since the EXAFS spectrum of that complex (23) was quite similar to those of our catalysts after sulfidation at 493 K. This is in turn again similar to MoS_3 which was recently shown to be formed by $Mo_3S(S_2)_3$ units (20, 35). Nevertheless, it cannot be completely excluded that the small Mo–S coordination numbers are simply due to a very disordered arrangement of the sulfur atoms around Mo.

The transition from the MoS_3-like phase to MoS_2 which involves the reduction of disulfide groups to sulfide ligands and/or H_2S was still not complete at 583 K and continued between 583 and 673 K during the sulfidation of the NiMo(NTA)/SiO_2 catalyst. In fact, the spectrum of the sample treated at 583 K did not show the characteristic features of MoS_2. It was still like the spectrum of the $[Mo_2(S_2)_6]^{2-}$ complex and the Mo–S and Mo–Mo coordination numbers were nearly equal to those obtained after treatment at 493 K (cf. Table 2). It is therefore likely that the H_2S production peak observed around 570 K for this and the other dried samples (Fig. 3) is at least partly due to the reduction of overstoichiometric elemental sulfur deposited on the surface, as proposed by some TPS studies (6–10), and not only

to the reduction of the MoS_3-like clusters as proposed by de Boer *et al.* (12), based on a combined TPS and EXAFS study of the sulfidation of MoO_3/SiO_2 catalysts. This conclusion would agree with the results of Wildervanck and Jellinek (36) who found that bulk MoS_3 loses sulfur above 523 K, but that crystalline MoS_2 is formed only above 623 K.

After treatment at 300 and 493 K the structure of Mo for the $NiMo/SiO_2$ catalyst was different from that for the $NiMo(NTA)/SiO_2$ catalyst, and was still dependent on the different original dried Mo phases (3). The Mo *K*-edge EXAFS of the $NiMo/SiO_2$ (Mo-first), $NiMo/SiO_2$ (Ni-first), and $NiMo(NTA)/SiO_2$ catalysts became equal (Fig. 6) after H_2/H_2S treatment at 673 K (the same temperature as that used for the sulfidation of the samples prior to the HDS experiments). Nevertheless, the HDS activities of the SiO_2-supported dried catalysts strongly varied as a function of the impregnation order and the addition of a chelating ligand (Table 1). It is therefore concluded that the differences in the thiophene HDS activities among the dried catalysts are not due to differences in their MoS_2 dispersion and that the influence of the chelating ligands on the MoS_2 structure of the working catalyst is marginal.

The sulfidation of the Ni atoms in the $NiMo/SiO_2$ (Ni-first) and $NiMo(NTA)/SiO_2$ catalysts differed substantially. The XANES and EXAFS spectra showed that the Ni atoms of the $NiMo/SiO_2$ catalyst became slightly sulfided at room temperature and that at 493 K no oxygen-first neighbors were present any longer (Figs. 7a, and 8a and Table 3). On the other hand, the $[Ni(NTA)(H_2O)_2]^-$ complexes in the $NiMo(NTA)/SiO_2$ catalyst were still present after sulfidation at 493 K (Figs. 7b, 8b). After sulfidation of the $NiMo(NTA)/SiO_2$ catalyst at 583 K, Ni–S and Ni–Ni distances of 2.24 and 2.8 Å respectively were observed. The Ni–S coordination number was high. Very similar results were reported by Crajé *et al.* (11) for a CoMo/C catalyst sulfided at 373 K. These coordinations do not match with any known bulk nickel or cobalt sulfide. It appears that the Ni (or Co) atoms are arranged in a special structure as soon as they are sulfided, and only later transform to Ni_3S_2 (or Co_9S_8) or to the "NiMoS" (or "CoMoS") phase. After 30 min of sulfidation at 673 K, the Ni EXAFS spectra of the $NiMo/SiO_2$ and $NiMo(NTA)/SiO_2$ catalysts also were quite similar, although small but significant differences were observed (Table 3). All Ni in the $NiMo(NTA)/SiO_2$ catalyst was in the "NiMoS" phase, whereas for the $NiMo/SiO_2$ catalyst some Ni_3S_2 was detected as well, suggesting that the smaller HDS activity of the latter is due to the lower "NiMoS" phase concentration, as proposed earlier by Topsøe *et al.* (37) and Wivel *et al.* (38) for $CoMo/Al_2O_3$ catalysts on the basis of Mössbauer emission spectroscopy and HDS results.

The present results and those of Crajé *et al.* (11) clearly show that the "NiMoS" (or "CoMoS") phase does not exist before Mo is in the form of well dispersed MoS_2 crystallites which are formed above 583 K only. When no NTA is present, Ni or Co are sulfided below 493 K, before the MoS_2 phase is formed. The resulting Ni or Co sulfide species slowly sinter to Ni_3S_2 or Co_9S_8, respectively, due to the weak interactions with the SiO_2 support, as shown (11) for carbon-supported catalysts. On the contrary, when NTA or EDTA is present, Ni is sulfided at higher temperature, between 493 and 583 K, just before the MoS_2 phase is formed. Hence, the chance of the Ni atoms being deposited on the MoS_2 crystallites and building the "NiMoS" phase, rather than sinter to Ni_3S_2, is higher.

The situation is different for γ-Al_2O_3-supported catalysts, since both the Ni^{2+} and the molybdate or heptamolybdate ions experience a strong interaction with the γ-Al_2O_3 surface (34). Therefore, small sulfided Ni agglomerates or single Ni atoms will have less tendency to sinter during sulfidation. As a consequence, calcined catalysts and samples prepared according to different procedures also have nearly the same activity as the NTA-based catalysts (Table 1).

CONCLUSIONS

The thiophene HDS activity of SiO_2-supported catalysts was found to be very sensitive to the mode of preparation. Calcination of the catalyst precursors led to a low dispersion of the active phase and to a relatively poor catalytic performance. Quite good catalysts were obtained when, in a sequential impregnation, the Ni was impregnated before the Mo salt, and when the Ni-first catalyst precursor was dried, but not calcined. A high catalytic performance was obtained by preparing the NiMo catalyst in the presence of chelating ligands, again without calcination.

The Mo *K*-edge EXAFS measurements on the dried catalysts confirmed that the sulfidation of the Mo atoms proceeds through a MoS_3-like phase. Although the sulfidation at low temperatures depended on the structure of the oxide Mo phase, the dispersion of the MoS_2 crystallites after treatment at 673 K did not depend on the preparation mode and thus did not correlate with the varying HDS activities.

The thiophene HDS activity did, on the contrary, correlate with the Ni phases present after sulfidation at 673 K. The Ni atoms in the catalyst made by sequential impregnation of Ni followed by Mo were present in the "NiMoS" phase as well as in Ni_3S_2, whereas in the NTA-based sample, which showed a better performance, Ni appeared only in the "NiMoS" phase. The positive influence of the chelating ligands was attributed to the stability of the $[Ni(NTA)(H_2O)_2]^-$ complex at temperatures up to 493 K against the very aggressive H_2S/H_2 mixture. Therefore, the Ni is sulfided just before the MoS_2 phase is formed and does not sinter to Ni_3S_2 but is deposited on the edges of the MoS_2 crystallites forming large amounts of the "NiMoS" phase. In contrast, when the Ni is already sulfided at low temperature, the nickel sulfide sinters to the thermodynamically stable Ni_3S_2 phase due to the absence of MoS_2.

These findings have important consequences for the design of new catalysts. The main objective should be to obtain a high dispersion of the MoS_2 phase as well as an ideal dispersion of the promoter atoms in the "NiMoS" or "CoMoS" phase. The MoS_2 dispersion is good for noncalcined catalysts but sensitive to the preparation procedure on a support like SiO_2, for which the support–precursor interactions are weak.

REFERENCES

1. Thompson, M. S., European Patent Application 0.181.035, 1986.
2. van Veen, J. A. R., Gerkema, E., van der Kraan, A. M., and Knoester, A. J., *Chem. Soc. Chem. Comm.* **1684** (1987).
3. Medici, L., and Prins, R., *J. Catal.* (1996).
4. Prada Silvy, R., Grange, P., Delannay, F., and Delmon, B., *Appl. Catal.* **46**, 113 (1989).
5. Prins, R., de Beer, V. H. J., and Somorjai, G. A., *Catal. Rev. Sci. Eng.* **31**, 1 (1989), and references therein.
6. Scheffer, B., de Jonge, J. C. M., Arnoldy, P., and Moulijn, J. A., *Bull. Soc. Chim. Belg.* **93**, 751 (1984).
7. Arnoldy, P., van den Heijkant, J. A. M., de Bok, G. D., and Moulijn, J. A., *J. Catal.* **92**, 35 (1985).
8. Arnoldy, P., de Booijs, J. L., Scheffer, B., and Moulijn, J. A., *J. Catal.* **96**, 122 (1985).
9. Scheffer, B., van Oers, E. M., Arnoldy, P., de Beer, V. H. J., and Moulijn, J. A., *Appl. Catal.* **25**, 303 (1986).
10. Scheffer, B., Arnoldy, P., and Moulijn, J. A., *J. Catal.* **112**, 516 (1988).
11. Crajé, M. W. J., Louwers, S. P. A., de Beer, V. H. J., Prins, R., and van der Kraan, A. M., *J. Phys. Chem.* **96**, 5445 (1992).
12. De Boer, M., van Dillen, A. J., Koningsberger, D. C., and Geus, J. W., *J. Phys. Chem.* **98**, 7862 (1994).
13. Crajé, M. W. J., de Beer, V. H. J., and van der Kraan, A. M., *Bull. Soc. Chim. Belg.* **100**, 953 (1991).
14. Schrader, G. L., and Cheng, C. P., *J. Catal.* **80**, 369 (1983).
15. Payen, E., Kasztelan, S., Houssenbay, S., Szimanski, R., and Grimblot, J., *J. Phys. Chem.* **93**, 6501 (1989).
16. Muijsers, J. C., Weber, Th., van Hardeveld, R. M., Zandbergen, H. W., and Niemantsverdriet, J. W., *J. Catal.* **157**, 698 (1995).
17. Louwers, S. P. A., and Prins, R., *J. Catal.* **133**, 94 (1992).
18. Bouwens, S. M. A. M., Prins, R., de Beer, V. H. J., and Koningsberger, D. C., *J. Phys. Chem.* **94**, 3711 (1990).
19. Bouwens, S. M. A. M., van Veen, J. A. R., Koningsberger, D. C., de Beer, V. H. J., and Prins, R., *J. Phys. Chem.* **95**, 123 (1991).
20. Weber, Th., Muijsers, J. C., and Niemantsverdriet, J. W., *J. Phys. Chem.* **99**, 934 (1995).
21. Brook, R. J., and Arnold, G. C., "Applied Regression Analysis and Experimental Design," p. 30. Dekker, New York, 1985.
22. Bronsema, K. D., de Boer, J. L., and Jellinek, F., *Z. Anorg. Allg. Chem.* **540/541**, 15 (1986).
23. Cramer, S. P., Liang, K. S., Jacobson, A. J., Chang, C. H., and Chianelli, R. R., *Inorg. Chem.* **23**, 1215 (1984).
24. Müller, A., Nolte, W. O., and Krebs, B., *Angew. Chem., Intern. Ed.* **17**, 279 (1978).
25. Müller, A., and Diemann, E., *in* "Comprehensive Coordination Chemistry" (G. Wilkinson, R. D. Gillard, and J. A. McCleverty, Eds.), Vol. 2, p. 515. Pergamon, Oxford, 1987.
26. Müller, A., Wittneben, V., Krickemeyer, E., Bögge, H., and Lemke, M., *Z. Anorg. Allg. Chem.* **605**, 175 (1988).
27. Bouwens, S. M. A. M., van Zon, F. B. M., van Dijk, M. P., van der Kraan, A. M., de Beer, V. H. J., van Veen, J. A. R., and Koningsberger, D. C., *J. Catal.* **146**, 375 (1994).
28. Bouwens, S. M. A. M., Koningsberger, D. C., de Beer, V. H. J., and Prins, R., *Catal. Lett.* **1**, 55 (1988).
29. Niemann, W., Clausen, B. S., and Topsøe, H., *Catal. Lett.* **4**, 355 (1990).
30. Fleet, M. E., *Am. Miner.* **62**, 341 (1977).
31. Bouwens, S. M. A. M., Koningsberger, D. C., de Beer, V. H. J., Louwers, S. P. A., and Prins, R., *Catal. Lett.* **5**, 273 (1990).
32. Louwers, S. P. A., and Prins, R., *J. Catal.* **139**, 525 (1993).
33. De Boer, M., van Dillen, A. J., Koningsberger, D. C., Geus, J. W., and Vuurman, M. A., *Catal. Lett.* **11**, 227 (1991).
34. De Boer, M., Leliveld, R. G., van Dillen, A. J., Geus, J. W., and Bruil, H. G., *Appl. Catal. A* **102**, 35 (1993).
35. Müller, A., Fedin, V., Hegetschweiler, K., and Amrein, W., *J. Chem. Soc. Chem. Comm.* **1795** (1992).
36. Wildervanck, J. C., and Jellinek, F., *Z. Anorg. Allg. Chem.* **328**, 309 (1964).
37. Topsøe, H., Clausen, B. S., Candia, R., Wivel, C., and Mørup, S., *J. Catal.* **68**, 433 (1981).
38. Wivel, C., Candia, R., Clausen, B. S., and Topsøe, H., *J. Catal.* **68**, 453 (1981).